Thermo-mechanical variability of post-industrial and post-consumer recyclate PC-ABS

Polymer Testing 99 (2021) 107216

Contents lists available at ScienceDirect

Polymer Testing

journal homepage: www.elsevier.com/locate/polytest

Thermo-mechanical variability of post-industrial and post-consumer recyclate PC-ABS

Eliott Orzan [a], Ratchawit Janewithayapun [a], Renaud Gutkin [b,c,*], Giada Lo Re [d], Kai Kallio [e]

[a] Department of Chemistry and Chemical Engineering, Chalmers University of Technology, Gothenburg, 41296, Sweden
[b] Safety Centre, Volvo Car Corporation, SE-405 31, Gothenburg, Sweden
[c] Department of Industrial and Materials Science, Division of Material and Computational Mechanics, Chalmers University of Technology, Gothenburg, 41296, Sweden
[d] Department of Industrial and Materials Science, Division of Engineering Materials, Chalmers University of Technology, Gothenburg, 41296, Sweden
[e] Sustainability Centre, Volvo Car Corporation, SE-405 31, Gothenburg, Sweden

ARTICLE INFO

Keywords:
Recycled
Polymer
PC-ABS
Mechanical properties
Thermal properties
Variation

ABSTRACT

The aim of this work is to investigate the performance variability of post-industrial (PIR) and post-consumer recycled (PCR) polycarbonate acrylonitrile-butadiene-styrene (PC-ABS). In addition, necessary testing methodology for understanding polymer variation in recycled polymers are established. The thermal expansion behaviour of all tested material were found to be similar and FT-IR testing revealed no conclusive evidence of oxidative degradation. Both PIR and PCR exhibited similar levels of variation in mechanical properties compared with prime samples, with the exception of elongation at break and quasi-static impact behaviour. In these two tests, prime polymers showed lower variation and superior performance to both recycled polymers. The presence of defects and changes in molecular weight were determined to be leading causes of the reduced deformability. Our work contributes by identifying key areas where recycled PC-ABS show good potential as replacements for neat PC-ABS. Furthermore, the work demonstrates methods for material testing against performance criteria to pave way for effective replacement of neat PC-ABS with its recycled counterparts.

1. Introduction

Plastics have become a contentious subject. They have become ubiquitous in every aspect of our lives but in recent years came under scrutiny due to a rising awareness of their polluting effect on the earth and its oceans. Industries and consumers will continue to produce and use plastics, respectively, so a collaborative effort should be made to find ways to re-use manufactured plastic and increase their time of use. The European Commission has set a strategy for plastics in a circular economy in 2018, announcing a goal of using 10 million tonnes of recycled plastics in new products on the EU market by 2025 [1]. This work aims to add knowledge to applications of recycled plastics in the automotive industry which accounts for 10% or 5.1 million tonnes/year of plastic demand in Europe [2].

Recycled plastics come in many forms. Post-Industrial Recyclates (PIR) are by-products of manufacturing processes that can be re-used in the manufacturing process [3]. Coming directly from production lines, these residuals are easily sorted thus ensuring a low-cost, high quality recycled material. It is important to distinguish PIR from in-factory scrap material, which are by-products re-granulated and re-fed within the manufacturing facility and not considered recycled content. Post-Consumer Recyclates (PCR) are plastic scraps generated by consumer end products that are collected by recycling plants and re-purposed [4]. These have the benefit of being sustainable and widely available but could suffer from inconsistent material compositions [3].

Polycarbonate/acrylonitrile-butadiene-styrene (PC-ABS) blends offer the most desirable properties of both components - the superior strength and engineering performance of PC and the high toughness at lower costs of ABS [5]. PC-ABS blends have found increasing use in the consumer electronics and automotive industries due to their excellent mechanical and thermal properties as well as good manufacturing processability [6]. These blends typically have high toughness, excellent ductility and impact toughness, good heat resistance and good melt viscosity [7,8]. However, there are many barriers and considerations that must be confronted to achieve a useful recycled polymer blend.

Polycarbonate is typically quite stiff but its processability is improved through the addition of ABS and other additives. Studies have shown that the rheological, mechanical and thermal properties change

* Corresponding author. Safety Centre, Volvo Car Corporation, SE-405 31, Gothenburg, Sweden.
E-mail address: renaud.gutkin@volvocars.com (R. Gutkin).

https://doi.org/10.1016/j.polymertesting.2021.107216
Received 1 December 2020; Received in revised form 19 April 2021; Accepted 22 April 2021
Available online 27 April 2021

through several reprocessing cycles. Re-processing of these materials can cause degradation, where shear and thermal forces during molding can lower the molecular weight. These materials were found to have lower T_g, impact strength, elongation at break and ductility [9]. Reprocessing can also deteriorate any additives use to improve miscibility and processability as well as introduce micro-contaminants to the blend. This, in addition to any degradation resulting from exposure to light, heat or water during use leads to a decrease in performance which is significant for companies concerned with product quality [10,11]. In fact, many companies believe that recycled materials do not meet their quantity and quality requirements and this issue could be regarded as a concern in the eyes of the consumer [12].

There exist many studies on recycling both post-consumer [13–16] and post-industrial PC-ABS blends [9]. As well as studies on possible methods to improve the compatibility, miscibility and performance of these blends [9,13–16]. However, to the best of the Authors' knowledge, there have been no detailed studies with larger sample sizes comparing the variability of prime, PIR and PCR PC-ABS polymers. The variability, or spread of values around the mean, of thermo-mechanical properties are a critical consideration in the application of recycled polymers. This is especially true within applications where reliability is essential; such as in automotive components. This work investigates commercially available prime, PIR and PCR PC-ABS where the suppliers have achieved a comparable performance to the prime polymers in their recycled blends. The aim is to quantify the levels of variation in prime and recycled polymers and compare them using statistical tools. The work will contribute by investigating the necessary methodology for understanding variability in thermo-mechanical properties of recycled polymers and whether these pose an issue when considering them as replacements for neat pristine polymers.

The approach taken has been to first characterize the polymers from each batch to investigate any variations in degradation, defects, molecular weight and composition. The characterization methods that will be used are ATR-FTIR, TGA, density, optical microscopy, SEM and oscillatory shear rheology. This is followed by thermo-mechanical testing to quantify the level of variation in each polymer type. Thermo-mechanical properties to be analyzed are based on common test routines for polymeric materials at Volvo Cars. These include tensile behaviour, impact behaviour and coefficient of linear thermal expansion (CLTE). Finally statistical tests in Levene's test, ANOVA and *t*-test are used [17–19]. Datasets are also checked for normality [20,21]. Levene's test is used to analyze differences in the variation of two data sets while the other two are for analyzing differences in the mean values. Using the proposed toolbox, determination of how recycled streams affect polymer performance can be assessed.

2. Experimental

PC-ABS material with recycled PC content from two suppliers were tested. Three batches of prime material from supplier 1 containing 50% PC was used as the benchmark. An equivalent grade material from supplier 1 with 50% PC, of which 90% are from recycled sources, was compared. Three batches of PCR PC-ABS containing 70% PC content, with all PC being from recycled sources, were obtained from supplier 2. From supplier 2's side, these three batches were chosen from batches that have some variability in their melt volume-flow rate (MVR) and Charpy impact tests, although still within standard tolerance limits. Furthermore, redundant or leftover stock PC-ABS products were reprocessed and added to batch PCR45. It is important to note that we are interested in the differences in the levels of inter-batch and intra-batch variation of prime, PIR and PCR materials. Comparisons of absolute values between prime and PIR materials are of interest to us, however the absolute values for PCR will be considered separately due to their higher PC content. In Table 1, the production field indicates whether the material has come from a production line (continuous) or were produced in the lab on a smaller scale. The numbers displayed next to the recycle type are supplier product numbers and do not describe any property of the material.

Table 1
Given and assessed PC-ABS material compositions.

Recycle Grouping	Given Composition	Assessed Composition[a]	Production	Individual Labels
Prime	50% PC	49% PC	Continuous	Prime 94 Prime 95 Prime 96
PIR	50% PC	50% PC	Lab Scale Lab Scale Continuous	PIR 97 PIR 98 PIR 99
PCR 27-28	70% PC	65% PC	Continuous	PCR 27 PCR 28
PCR 45	70% PC	55% PC	Continuous	PCR 45

[a] Estimated from density, inorganic residual <2% by TGA.

2.1. Polymer variation analysis

2.1.1. FT-IR

Analysis were made using Fourier-transform Infrared Spectroscopy (FT-IR). Measurements were made in Attenuated Total Reflection (ATR) mode in the Nicolet iS50 FT-IR with 16 scans and 4 cm^{-1} resolution. Environmental background was measured prior to every new sample collection.

2.1.2. Density

Density measurements were performed in a Mettler Toledo AX204. Small cuts of samples were cut from a plate and their weights were measured in the instrument. Then, the volume of the cut sample was measured by placing it into a sample holder in anhydrous ethanol.

2.1.3. Rheology

Rheological properties were determined using a Discovery HR-2 rotational rheometer. The measurements were carried out using a plate-plate configuration with shear rate range of 0.1–100 rad/s at 200°C. A strain amplitude sweep was performed and 10% strain was chosen as representative for the linear viscoelastic region. The soak time was set at 20 s after which continuous oscillation occurred for 600 s.

2.1.4. Scanning electron microscope (SEM) and energy-dispersive X-ray spectroscopy (EDS)

Measurements were conducted in a JSM-IT300 instrument at 15.0 kV and 50 Pa vacuum pressure. Fracture surfaces were mounted onto a conductive platform and analyzed without any coatings as images of the surface were obtained with good resolution.

2.1.5. Thermal stability and filler content

Analysis was made using Thermal Gravimetric analysis (TGA). Measurements used small cuts of polymer samples weighing approximately 20 mg. Measurements were performed in a Mettler Toledo TGA/DSC 1 instrument. Experimental conditions were 25 °C/min, N2 flow 55.0 mL/min from 25°C to 600°C. Then, kept at 600°C for 5 min before being heated up from 600°C to 900°C at a rate of 10°C/min with O_2 flow of 55.0 mL/min.

2.2. Thermo-mechanical characterization

2.2.1. Tensile properties

Three tensile parameters are chosen for analysis: Young's modulus, yield strength, and plastic onset. After initial experiments, it was observed that the materials displayed an unusually high variation in the elongation at break. Therefore, this was added as the fourth property for analysis and is meant to give a measure of the materials' tensile toughness.

Dog bone shaped samples according to ISO 527-2 model 1A were used [22]. The samples had a thickness of 4 mm except for PCR28, where samples of thickness 4.4 mm were received from the supplier. Tests were performed in a Zwick Roell instrument equipped with an optical extensiometer and a 10 kN load cell. The instrument set-up parameters were: gauge length of 50 mm, 10 N pre-load force, an initial speed of 5 mm/min for young's modulus determination, and secondary speed of 50 mm/min from 1% strain onwards. The secondary speed was used to ensure that samples break within a reasonable amount of time. Experiments were performed at room temperature. Testexpert II software was used for analysis and Young's modulus was calculated from 0.25 to 1% strain using the secants method, plastic onset was taken as 0.2% plastic strain and yield stress can be obtained directly from the program. The Young's modulus was chosen at these two points to avoid an equipment induced bump at 0.1% strain, and the wider range gave a better consistency. The plastic onset was taken at 0.2% likewise, to improve consistency by ensuring that the polymers are showing plastic behaviour at the measured point. For determination of elongation at break, the crosshead travel and the entire narrow section was used for gauge length (80 mm). This was to account for strain occurring outside of the optical extensiometer gauge length. At least 15 samples of each batch were tested (with more samples tested where needed), with exception of elongation at break where only 7 to 10 data points from each batch were measured.

2.2.2. Impact

Fracture initiation energy is commonly used to evaluate the impact performance of polymeric materials [23,24]. Two methods for evaluating impact fracture behaviour were initially evaluated: falling-dart and quasi-static testing. However due to inconclusive data from falling-dart tests, the experimental setup and results of that method are found in Appendix A.1. Experimental theory for both impact tests can also be found in Appendix A.1.

Sample PC-ABS plates with a thickness of 2 mm were centered and fixed between two 3 kg steel plates and secured with 15 N of force through 4 bolts on each side of the sample. A dart with a diameter of 2 cm was slowly pushed into the center of the plate at a rate of 5 mm/min until fractured.

2.2.3. Coefficient of linear thermal expansion (CLTE)

Dogbone tensile samples were first conditioned at 110°C overnight to remove effects from residual stresses. Then, they were fixed onto a frame as shown in Fig. 1. A piece of kevlar fiber was then glued to the far end of the sample and looped around a high precision MTS extensiometer (detection range of 15 mm). A small weight was attached at the end of the looped kevlar to keep the fiber taut. Lastly, a temperature probe was fixed onto the sample surface. The setup described was then placed in a climate chamber and cooled to −30°C for 1.5 h. Then the temperature was increased by 1°C/min to 110°C. The extensiometer and the temperature probe are linked to a Dewesoft instrument where data from both was logged at a rate of 1 Hz (1 point per second). Any expansion or contraction of the sample pushed or pulled the kevlar fiber and was read by the extensiometer. By plotting the change in displacement vs temperature, a coefficient for linear thermal expansion can be calculated. The equation used and subsequent results can be found in Appendix A.3.

2.3. Statistical analysis

Two different programs were used to run statistical analysis, Python and IBM SPSS. Python was used to run the normality tests: D'Agostino's K-squared test [20] and the Shapiro-Wilk test [21] using the scipy.stats module from the Scipy library [25]. SPSS was used to run ANOVA [18,19], Levene's test [17] and t-tests or the non-parametric equivalent Welch's *t*-test [19]. A confidence interval of 95% is used, meaning the alpha value to compare resulting p-values is set at 0.05. Prior to analysis, outliers outside of 3 standard deviations from the mean in data were removed.

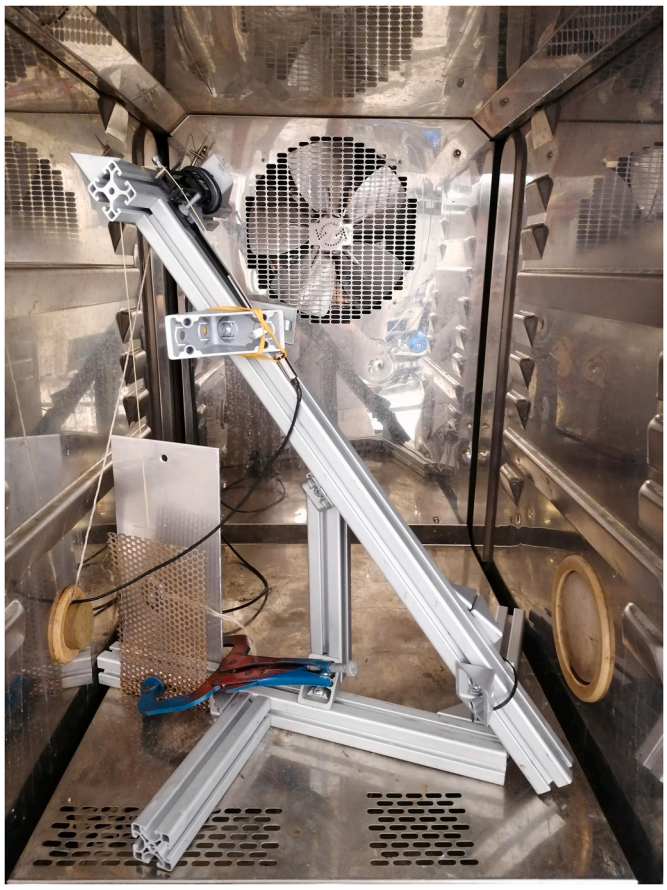

Fig. 1. Experimental setup for CLTE experiments.

3. Results and discussion

3.1. Composition assessment

Suppliers of the PC-ABS blends each gave three different batches of each material, having properties within the acceptable threshold for their production standards. As the ratio of PC to ABS heavily influences the properties of the PC-ABS blend [5,26,27], preliminary steps to estimate the blend compositions were taken. Equation (1) can be used to estimate the percentages of PC and ABS (Table 1) using the experimentally measured densities of the different blends and the reference densities of PC and ABS. PC and ABS have only partial miscibility which has been shown to cause some deviation from the equation, but the extent is less than 5% [27]. The inorganic content has been analyzed by TGA to be less than 2 w% (see Section 3.8) and therefore, should not affect the calculations.

$$\frac{1}{\rho}=\frac{w_1}{\rho_1}+\frac{w_2}{\rho_2} \tag{1}$$

To ensure the validity of the density-estimated composition, another test method was performed, in which the intensity of certain ATR-FTIR peaks in PC-ABS can be correlated to the percent of PC in the blend [28]. The peak at 697 cm^{-1} is a characteristic peak of ABS (aromatic C–H out of plane angular deformation) and was chosen as a reference, while the intensity of the characteristic peak for PC at 829 cm^{-1} (aromatic C–H angular deformation) [28] was used to compare PC to ABS ratios. These two peaks were selected as they do not overlap between PC and ABS and had lower baseline normalization errors due to being closer to each other. They are also not affected by possible degradation products or

other additives in the polymer blend [8,15,28].[1]

Fig. 2b shows a magnified image of this peak for PCR samples. Since the intensity of the PCR45 PC peak is lower, we can conclude that there is less PC in it than in PCR27-28. IR spectra and the PC peak intensities for each sample can be found in Appendix A.4. The same comparison was performed between the ABS 697 cm^{-1} peak and the more recognizable PC 1775 cm^{-1} peak (C═O axial deformation) and the same trends were observed (refer to Table A.6 in Appendix A.4). A correlation between the PC-ABS IR peak intensity ratios and the blend density found in experiments was used to estimate PC-ABS composition. Fig. 2a shows that the correlation between the IR ratio and density is strong with an R-squared value of 0.978.

Comparison between experimental and given densities from suppliers indicates a good match, thereby providing support for the validity of our methods. The PCR45 batch was significantly different however. This batch was confirmed by the supplier to contain leftover stock PC-ABS products. As a result, we expected PCR45 to behave differently from the other PCR batches in thermo-mechanical tests and considered it separately from PCR27-28 in tests.

3.2. Tensile results

Data collected for the prime, PIR and PCR27-28 and PCR45 samples were grouped according to their recyclate types and PC to ABS ratio (Fig. 3b). The data was analyzed using Levene's test for homogeneous variances and the *t*-test for mean variation. A statistically significant difference in the Levene's test can highlight intra-batch and inter-batch variation. Table 2 summarizes the findings.

3.2.1. Comparisons of PIR against prime material

Levene's tests for parameter variability showed that variation of yield stress in PIR samples was the only parameter statistically different from the prime. Moreover, deeper analysis showed that yield stress variation in the prime material was greater than that of the PIR (Table 2 and Fig. 3a). In this parameter, all batches of prime material were actually found to be statistically different from each other. Variation of tensile parameters in PIR should therefore, not pose a problem in practical applications.

Since PIR was designed as an alternative for the prime material, the mean values of their tensile properties were also compared. A statistical difference was found only in the mean plastic onset values. This difference was then investigated using the non-parametric version of ANOVA.[2] Prime95 and PIR99 were found to be the upper and lower bound respectively. As it is only between these two batches where a statistically significant difference is found, the means of all the prime and PIR samples are not so different. This is also observed in the box and whiskers plot for plastic onset (see Fig. 9b in Appendix A.2).

In summary, PIR samples performed similarly to the prime materials in the tested parameters and the slight differences should not affect the overall performance.

3.2.2. Comparisons of PCR against prime material

Initial comparisons between the prime and the PCR material showed a statistically significant difference in variance for every material property. Due to the PCR batches including PC from consumer end-use sources, we expected a higher variation in our results. However, ANOVA tests on the whole PCR group showed that the results had been affected by the behaviour of PCR45 due to its different PC to ABS ratio. Therefore, we isolated the PCR45 in all further recyclate comparison tests.

After isolating batch PCR45 from the groupings and rerunning the tests, the two groups (PCR27-28 and PCR45) still showed higher variation in Young's modulus and plastic onset than the prime although to a much smaller degree. The two properties suffered from high intra-batch variation. The difference in variance in plastic onset was not found to be statistically significant for the PCR27-28 group, yet remained significant for PCR45. Furthermore, the variation of yield stress for both PCR27-28 and PCR45 were also found to be significantly lower than that of the prime samples.

These differences are well visualized in Fig. 3a. While the variation of Young's modulus and plastic onset is higher in PCR27-28 compared to the prime, this should not pose a problem in practical applications as the variations are small in comparison to the parameter values. The larger variation and drastic change in behaviour of the PCR45 however, may require further matching of properties to design criteria. This also demonstrates the importance of being able to identify such outlier batches.

3.2.3. Elongation at break

Within elongation at break, many significant observations were made (Fig. 3b). First, the ductility for the tested prime and PIR samples were much higher than expected. Values for a 50% PC blend have been reported to be 20% [27], 12% [26] and 20% [5]. Furthermore, it has been reported that the elongation at break of PC-ABS blends decrease with increasing ABS content. The minimum value was found at approximately 50% PC [5,27] due to poor interphase interactions at this composition [27]. In the mentioned literature, the elongation at break for a 70% PC blend were 22% [27], 10% [26] and 22% [5]. From these data, the elongation at break for a 70% PC blend should be similar to or higher than for a 50% PC blend. Even after taking into consideration their different manufacturers, the difference is still large enough to warrant further investigation.

It can also be seen that recycled content has a significant effect on the mean and variation of the elongation at break. The mean value for the PIR samples is 15% lower than that of the prime while the standard variation is 140% higher. Here, the difference in mean was not found to be statistically significant while the variation was significantly different. Similarly, PCR45 is also affected by its different recycled content composition compared to PCR27-28. PCR45 exhibited a 46% higher elongation at break and a 54% higher variation compared to PCR27-28. The former is likely due to its lower PC content and the latter due to higher contamination in the blend. Here, the mean difference was statistically different while the variation was not. Interestingly, the PCR27-28 group displayed lower variation than the prime material. While this is a positive result, the unusually low elongation at break could mean defects or inter-phase interactions have caused all samples to fail right after necking. As such, in later experiments, the fracture surfaces were analyzed and the toughness in impact testing were also considered.

3.3. Fracture surface analysis

The fracture surfaces of prime samples studied under optical microscope were free of defects as shown in Fig. 4a_1. However, defects consisting of cavities or embedded particles of varying sizes are observed in PIR and PCR samples. Observed defects were categorized based on diameter into small: 100 μm, medium: 300–500 μm and large: >700 μm .

The size of ABS domains within polymer blends are typically much smaller at 5–10 μm [29,30] compared to defects observed in our samples. According to suppliers' specifications, particles larger than 100 μm are filtered out through a mesh. This rules out the possibility of the defects being artifacts from larger contaminants in the blend. Therefore, the larger defects can be ascribed to pull out of larger ABS domains. It is hypothesized that a poor dispersion of the ABS domains led to the agglomeration of the domains, resulting in the observed cavities upon

[1] This ratio does not correspond directly to the %PC/%ABS. A calibration curve would be needed to interpolate the %PC/%ABS from the ratio.

[2] This was done because some of the datasets were not normally distributed and the sample sizes were not large enough to justify applying the central limit theorem.

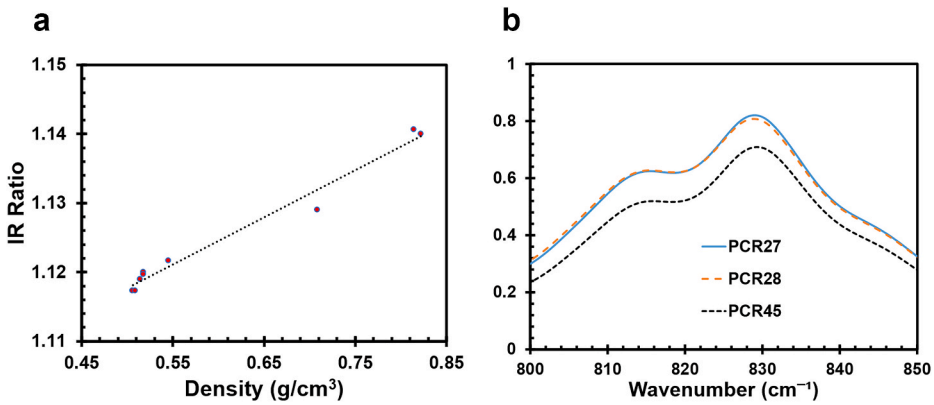

Fig. 2. Correlation between PC-ABS IR ratio of intensities at 829 cm^{-1} peak and density values, $R^2 = 0.978$ (a). Normalized ATR FT-IR spectra of PCR PC-ABS, with the 827 cm^{-1} region expanded (b).

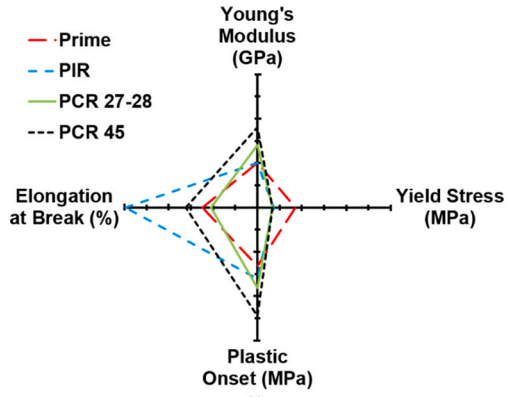

(a)

Sample	Young's Modulus (GPa)	Plastic Onset (MPa)	Yield Stress (MPa)	Elongation at Break (%)
Prime	1.88 ± 0.10	41.71 ± 1.32	48.50 ± 0.86	134.74 ± 12.43
PIR	1.91 ± 0.10	40.95 ± 1.61	48.32 ± 0.37	114.43 ± 29.78
PCR27-28	2.05 ± 0.14	44.01 ± 1.82	56.48 ± 0.34	23.77 ± 10.48
PCR45	1.94 ± 0.18	41.93 ± 2.45	50.90 ± 0.34	34.79 ± 16.12

(b)

Fig. 3. Comparisons of variability for all tested tensile properties (a). Tensile properties of tested PC-ABS (b).

Table 2
Summary of results for Levene's statistical tests for variance in tensile tests. All entries are whether there is a statistically significant difference in variance when compared against prime samples.

	PIR	PCR	PCR 27-28	PCR 45
Young's Modulus	No	Yes	Yes	Yes
Plastic Onset	No	Yes	No	Yes
Yield Stress	Yes	Yes	Yes	Yes

fracture. This could be a result of a change in the miscibility of PC and ABS phases, or an ineffective dispersion during melt compounding.

PIR samples showed fracture surfaces similar to that of the prime samples, albeit with some frequency of medium sized defects. However, in some other cases (Fig. 4b), the PIR samples showed large defects which likely acted as a point for fracture initiation and propagation. Within the PCR samples (Fig. 4d), we observed much higher size and frequency of all defects, especially in PCR45. Furthermore, we observed fracture patterns around some of the small to medium sized defects as seen in Fig. 4c. In some cases, these particles had remained in the cavities after fracture and were observed to be shiny, metallic particles (Fig. 4f).

Investigations with SEM and EDS revealed these particles to be aluminum which is not an expected part of the PCR blend and are possible contaminants from the manufacturing process, recycling process or recyclate source according to the supplier (Fig. 4c). Additional contamination from salts, clay and other particles such as titanium were found in all recycled polymers.

The table in Fig. 4 summarizes the average number of defects found in each sample. The higher frequency of defects found in the recycled polymers are thought to be one of the primary causes for the lower elongation at break in the tests as they can act as initiation points for fracture. Where there is a consistently high occurrence of defects, as in the PCR samples, then all the samples are likely to fracture after necking, resulting in a much lower mean elongation at break and also a lower variation. With a lower number of defects as in the PIR samples, the mean elongation at break is less affected but the variation would increase from samples where a defect has initiated a fracture at lower strains.

3.4. Quasi-static impact results

A quasi-static impact test provides precise data which can be used to understand toughness differences between polymers. For the sake of completion, we have also done a falling-dart impact test. However, due to large variations from the testing method (see Appendix A.1), material variation could not be distinguished and the quasi-static impact test was preferred.

Both the prime and PIR materials behaved as expected, deforming more and having a higher toughness due to its higher percentage of ABS (Fig. 5). Samples of prime material deformed the most, and sustained the highest load before fracturing. The PIR materials performed significantly worse. They sustained a much smaller maximum load and deformation compared to the prime. Furthermore, the mean fracture energy was 16.1% lower with a higher level of variation. A Levene's test indicated that the variances between the prime and PIR are still statistically similar however.

When comparing the PCR batches to prime, the variation was also found to be high but still statistically similar. The fracture energy for PCR samples was much lower than prime or PIR, which was expected considering the percentage of PC in these batches is higher. Interestingly, the PCR45 had a similar mean and variation compared to PCR27-28, indicating that PCR45 has a much lower impact resistance than expected for its composition and factors other than the composition are dominant in causing the lower toughness. Thus, it is hypothesized that the higher frequency of defects in PIR and PCR are the primary causes for lower fracture energies. These results also agree with findings in elongation at break tensile tests. The ductility of the materials in tension showed similar trends to the fracture energy and displacement.

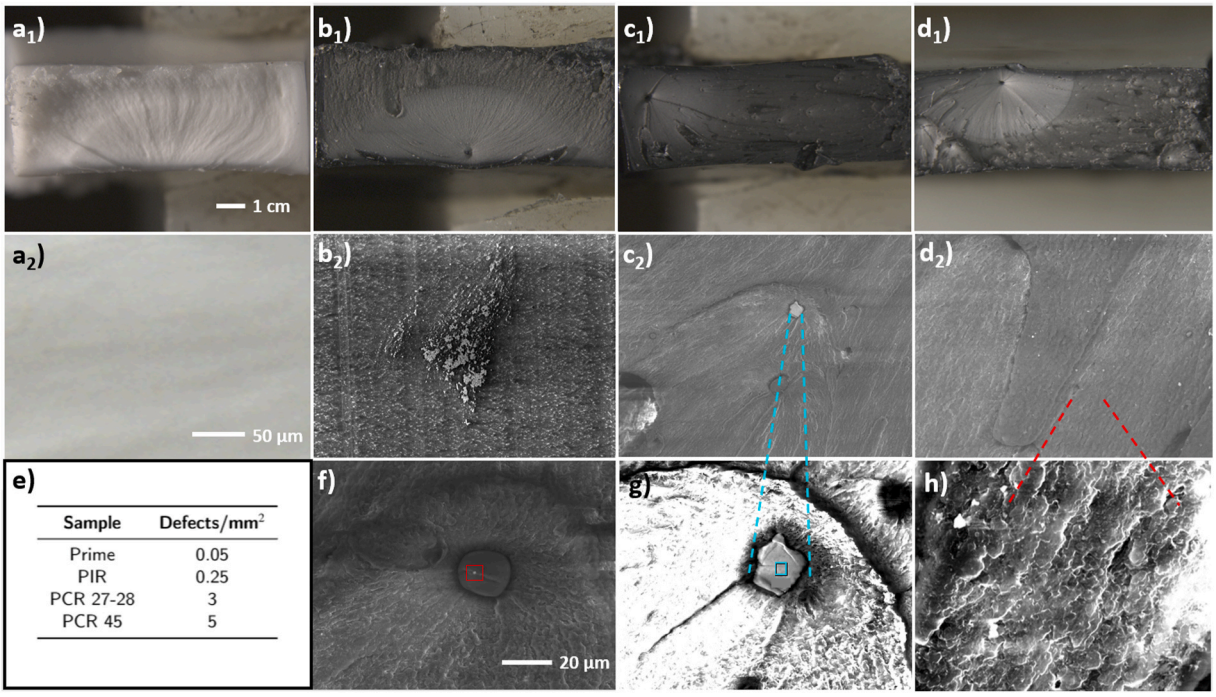

Fig. 4. Series of figures showing tensile fracture surfaces under optical microscopy for Prime (a_1), PIR with salt contamination(b_1), PCR27-28 (c_1) and PCR45 (d_1). SEM magnification reveals surface structures in the same sample order for the second row. Total defects/mm^2 are shown in (e). (f) and (g) show magnified SEM images of visible inclusions of ABS agglomeration and an aluminum particle in PCR 27. The red square in (f) is confirmed to be aluminum as well. Close PCR 45 morphology can be seen in (h). Note that inorganic residues were found to be below 2% in TGA analysis. (For interpretation of the references to colour in this figure legend, the reader is referred to the Web version of this article.)

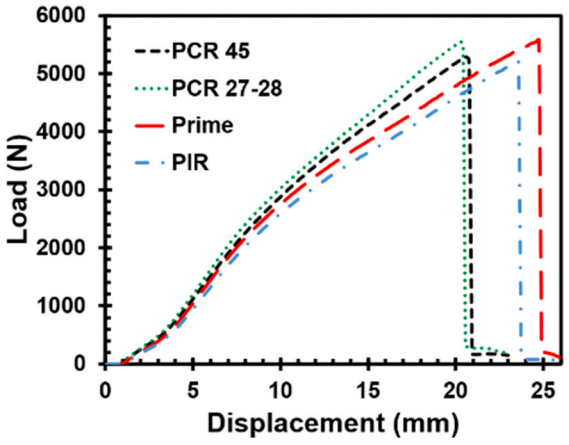

(a)

Sample	Fracture Energy (kJ)	Maximum Load (N)	Displacement (mm)
Prime	75.63 ± 3.72	5589	24.7
PIR	63.43 ± 5.78	5186	23.1
PCR 27	56.09 ± 5.61	5466	19.9
PCR 45	56.85 ± 4.92	5265	20.6
Significance Values:		ANOVA: 0.00	Levene's: 0.603
Notes: Only 27 and 45 have similar means			

(b)

Fig. 5. Quasi-static impact test force vs displacement graph (a). Quasi-static impact testing data (b).

3.5. CLTE results

Thermal expansion in polymers is an important design criteria in applications where fluctuations in heat are common (such as cars in this instance), and thus is statistically analyzed as shown in Table 3. Levene's test and ANOVA showed no inter-batch variation between all samples. Further analysis in Appendix A.3 found that PIR and PCR showed no difference when compared to the Prime samples.

3.6. Infrared Spectroscopy

IR techniques can be used to characterize PC-ABS degradation. Rajan et al. [8] used the broad peak at 1713 cm^{-1} which is ascribed to carbonyl groups in aliphatic acids, which were not present prior to ageing, as a measure of photo-oxidation. It was mentioned that polycarbonate degrades to produce peaks mainly in the carbonyl region (1600–1800 cm^{-1}) while ABS degradation produces peaks in the carbonyl (1600–1800 cm^{-1}) and hydroxyl region (3200–3600 cm^{-1}) due to oxidized moieties formed from degradation of the polybutadiene [8,15].

There is no conclusive evidence for oxidation degradation within our PIR and PCR samples. In Fig. 11, the spectra of both PIR and PCR material did not show additional peaks in the 1713 cm^{-1} (aliphatic acid

Table 3
Coefficient of thermal expansion data for recyclate types.

Sample	$\alpha(m/m^*C)*10^{-5}$
Prime	7.73 ± 0.19
PIR	7.93 ± 0.22
PCR 27-28	7.59 ± 0.17
PCR 45	7.53 ± 0.02
Significance Values:	
ANOVA: 0.05	Levene's: 0.059

carbonyl groups) or in the 3500 cm^{-1} (hydroxyl and acid groups) ranges compared to the prime [8] (refer to Appendix A.4).

3.7. Rheology

Rheological assessment is an efficient method to determine differences in molecular weight (MW), molecular weight distribution (MWD) and is much more sensitive than TGA towards differences due to degradation. As a polymer undergoes degradation, the polymer chains break apart, causing a decrease in the MW and an increase in the MWD. Rheological testing using oscillatory shear measures viscosity, loss modulus and storage modulus and provides insight into the behaviour of the viscoelastic polymer melt. With a higher MW, polymer chain entanglements increase and thus the viscosity of the melt also increases [31]. The crossover point between curves of loss and storage moduli determines where a polymer melt will go from primarily elastic (higher storage modulus) behaviour to a more viscous (higher loss modulus) response [32]. A higher crossover frequency indicates a lower molecular weight while a higher crossover modulus indicates a narrower MWD [31–33]. Viscosity and elastic (storage) modulus also reflect the different ratio of components in the PC-ABS blend. With a higher percentage of PC, the viscosity and crossover modulus increase accordingly [26]. Representative curves of the main rheological properties are shown in Fig. 6a, while an overview of the rheological results are summarized in Fig. 6b and Fig. 6c.

Comparison of prime to PIR samples revealed they were statistically similar in both mean and variation for crossover frequency and viscosity. This suggests a similar average molecular weight between the two. However, a statistically significant difference for both mean and variation in crossover modulus indicates both a broader MWD and a lower stiffness in the PIR.

Similar to previous tests, we observed that PCR27-28 differ significantly from PCR45 in all parameters. A higher complex viscosity and a higher crossover modulus in the PCR27-28 can both represent the higher PC content. Thus, no conclusion about differences in MWD can be made. However, the lower crossover frequency observed in conjunction with the higher viscosity suggests a higher MW in the PCR27-28. The variation within all three parameters are larger in the PCR27-28 which is likely related to their higher recycled PC content.

In terms of viscosity, the PCR samples are much lower than was expected considering their PC content. As a 55% PC blend, PCR45 is expected to have a similar viscosity when compared to prime and PIR. This suggests that the MW of both the PCR samples may be lower than the prime and PIR, which can be attributed to the different source materials, ageing effects, and processing parameters. It has been reported that re-processing of polymers may induce thermo-mechanical degradation [34], leading to a broadening of the MWD. Other factors such as long polymer branching and fillers are expected to increase the viscosity of the blend [31].

3.8. Thermal stability

Degradation may be a result of shear and thermal stresses during reprocessing or ageing effects in the source material, which can be traced by TGA. A lower onset degradation temperature could indicate a lower MW in the batch [9]. This trend can be seen in Fig. 7a, as the onset degradation temperature for PCR samples are lower than prime and PIR. With a higher percentage of PC, the thermal stability of the blend was expected to increase. Therefore, the lower onset temperature is a possible indication of lower MW and broader MWD in PCR samples. A larger fraction of recycled PC in the PCR blends could contribute to a

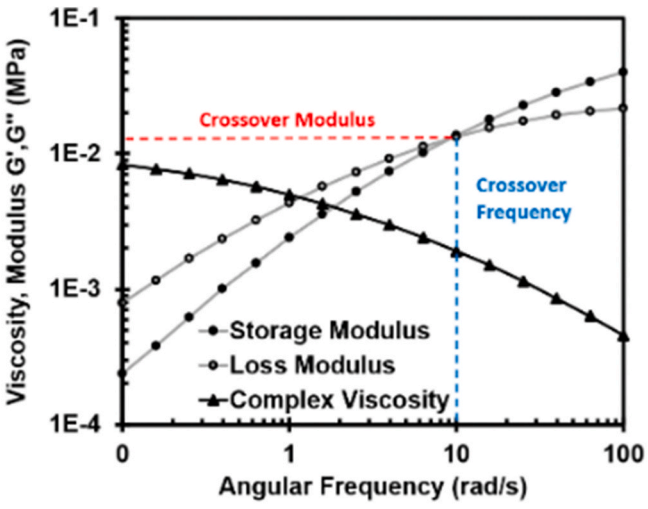

(a)

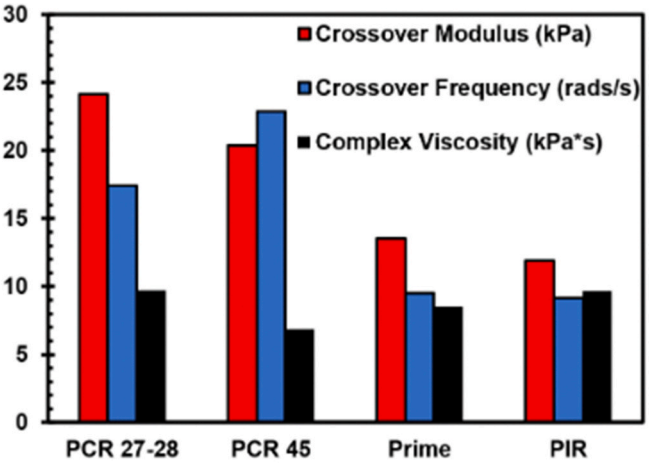

(b)

Sample	Crossover Modulus (kPa)	Crossover Frequency (rad/s)	Complex Viscosity (kPa*s)
PCR 27	24.13 ± 2.58	17.43 ± 0.73	9.69 ± 1.37
PCR 45	20.38 ± 0.57	22.87 ± 0.51	6.83 ± 0.34
Prime	13.53 ± 0.57	9.49 ± 0.24	8.53 ± 0.28
PIR	11.91 ± 1.35	9.16 ± 0.32	9.18 ± 0.62
Prime vs PIR Significance Values			
ANOVA	0.023	0.125	0.079
Levene's	0.00	0.239	0.372

(c)

Fig. 6. Rheological test results: Representative frequency sweep curves for viscosity, loss and storage moduli (a), Overview of main oscillatory shear rheology results (b), and summary of main rheological data (c). The crossover point refers to the intersection between the loss and storage moduli curves.

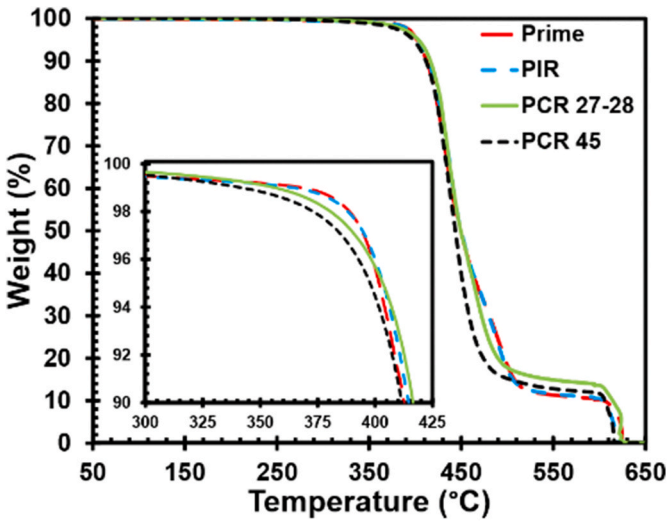

(a)

	T2% (°C)	Residual % at 800°C
Prime	388.8	0.67
PIR	388.1	0.94
PCR 27-28	380.5	1.68
PCR 45	373.0	1.36

(b)

Fig. 7. Representative TGA curves for each material (a)and table showing degradation onset temperature at 2% weight loss and residuals after oxidation at 600–800°C (b).

broadening of the molecular weight distribution. On the other hand, there were no differences between prime and PIR.

As the samples undergo combustion between 600 and 800°C, less than 2% of material remained as residuals (Fig. 7b). SEM-EDS analysis of the residuals revealed that the majority of the residuals was composed of titanium (Ti) and oxygen (O). In addition, iron (Fe) particles and zinc (Zn) particles in PIR samples approximately 200 μm in diameter were found. While in PCR samples, larger flakes composed of Ti and O of approximately 200 μm in diameter were observed. Interestingly, the aluminum particles observed in the fracture surface were not present in the tested samples, suggesting outside contamination. The residuals shown in Fig. 7b confirm the non-negligible increase in contamination from re-processing or use that likely affected the fracture variability of the recycled materials.

4. Conclusions

With the aim of evaluating the performance of polymers from recyclate streams to replace prime polymers in automotive parts, variation within PC-ABS blends of prime, and PIR and PCR recyclate types were analyzed. In tested thermo-mechanical parameters, both PIR and PCR exhibited comparable levels of variation compared to the prime with the exception of elongation at break and quasi-static impact behaviour. In these, the PIR showed a significantly lower toughness and higher variation compared to the prime despite having similar blend compositions. The levels of variation in the PCR quasi-static tests were also elevated, beckoning more detailed investigations into the causes.

To explain differences in performance between the materials, analysis on blend composition, defects and degradation were performed. Morphological analysis of tensile fracture surfaces through SEM and optical microscopy revealed significant defects in the PIR and PCR samples. These defects were found to be cavities of ejected ABS domains and on some occasions contaminants or agglomerated inorganic additives. The reduced deformability of PIR and PCR samples were found to be correlated to the size and frequency of defects. While no conclusive evidence of oxidative-degradation were found in the FT-IR analysis, TGA and rheological measurements indicated significant changes in molecular weight and molecular weight distribution compared to the prime. The variation in these tests was also higher, as expected with a higher recycled PC content. In conclusion, anomalies in blend composition, the presence of defects, and variation in molecular weight and molecular weight distribution are the major contributors to the toughness differences observed in the PIR and PCR samples.

From a batch variation point of view, both PIR and PCR do not differ significantly from the prime PC-ABS except in toughness and can be considered suitable replacements in applications where toughness is not a critical parameter. Otherwise, further investigations such as those undertaken in this work are recommended and modification of the blend may be required. Many of the challenges of recycled materials are inherent and cannot be avoided. Therefore, tuning of processing parameters based on good knowledge of the source materials is paramount in controlling changes in morphology and composition. This would allow for much wider applications of recycled polymers within the automotive industry and other industries.

Declaration of competing interest

The authors declare that they have no known competing financial interests or personal relationships that could have appeared to influence the work reported in this paper.

Appendix

A.1. Falling-Dart Impact Testing

In a falling-dart impact test, a dart indents a fixed flat polymer plate after free-falling from an elevated position. In a quasi-static impact test, the dart is slowly indented into the center of the plate at a constant velocity. The objective is to evaluate the energy absorbed by the plate through a force transducer inside the dart and measuring its displacement over time. This energy is analogous to how the polymer deforms and fractures due to its strain-rate dependent elastic and plastic behaviour. The total energy absorbed is a sum of the spring-like elastic components and permanent plastic deformation. It can also be divided into the fracture initiation energy and crack propagation energy. To determine fracture initiation energy, a polymer plate is impacted with excess energy (or high velocities in a falling-dart test), causing it to fracture. On a force-time or force-displacement curve, the fracture initiation energy is denoted by a sudden decrease in the load on the impact dart [35]. The amount of energy absorbed or fracture energy can be found by calculating the area under the curve of a force-displacement graph until the point of the sudden drop-off.

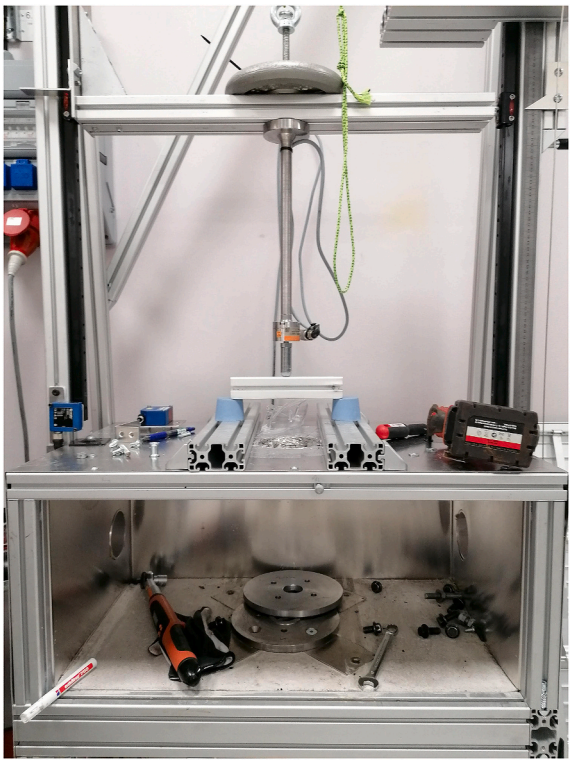

Fig. 8. Experimental setup for falling-dart impact tests.

It is well documented that falling-dart impact testing is not useful to understand sample to sample variations [23]. The troubles with data acquisition in such a short time-frame makes any analysis regarding the damage initiation and evolution difficult [36]. And while there is debate regarding whether low velocity impact tests provide similar results to quasi-static tests [36–39], our results confirm that these two methods are not equivalent. The mean fracture initiation energies and variation are not the same between the two tests. In addition, quasi-static tests reveal statistically different fracture energies between each sample while falling-dart does not.

During testing, it was found that various errors resulting from the apparatus such as inaccurate position and force readings, coupled with friction in the descent of the falling dart furthered the inaccuracy of this measurement technique. The scattering in the data was high, causing large variation in the data, making it difficult to draw proper conclusions about variability between materials. Quasi-static tests show less scattering in the data, was a more controllable test, and produced deformation data that could be used to distinguish differences between a prime and PIR batch.

The results are shown in Table 4. Statistically there is no mean difference between the samples. Visually, prime samples have a higher fracture energy and variability compared to the recycled plates. According to Levene's test, PIR samples had a similar variability to PCR and prime polymers. However, PCR variability was statistically lower than prime samples. Within PCR samples however, we found that PCR45 had a degree of variation closer to that of the prime samples compared to batches of PCR27 and PCR28.

Table 4
Falling-dart impact fracture energies and 95% confidence intervals

Sample	Mean Energy (kJ)	Levene's Test	
Prime	56.69 ± 2.96	vs PIR	0.19
PIR	54.10 ± 2.14	vs PCR	0.327
PCR	52.73 ± 1.51	vs Prime	0.001

A.2. Tensile Testing

Young's modulus is a measure of a material's stiffness in the elastic region, while plastic onset is used to provide information on where the material starts to exhibit plastic behaviour. Finally the yield strength indicates the point where the polymer starts to form a neck and the start of strain hardening behaviour [24,40].

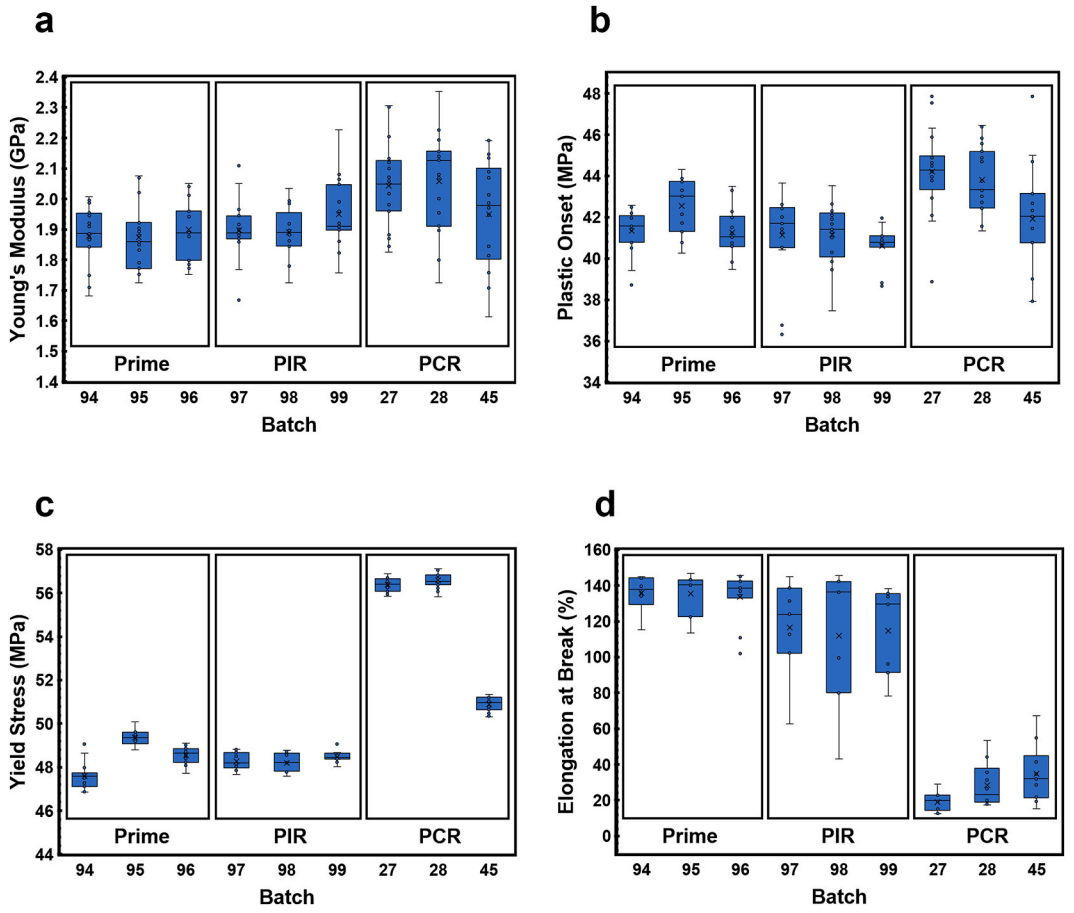

Fig. 9. Box and whisker plot of tensile properties. Young's modulus (a), plastic onset (b), yield stress (c) and elongation at break (d).

A.3. CLTE

CLTE ($\frac{m}{m \cdot C}$) describes the expansion and contraction behaviour of a material in one direction in response to temperature changes. The coefficient is given in Equation (2) where α can be estimated as the slope of the linear section in a displacement vs temperature curve if the slope does not change with temperature.

$$\alpha = \frac{1}{L_0}\frac{dL}{dT} \tag{2}$$

Table 5
Significance values for inter-batch and inter-recyclate variation for coefficient of thermal expansion.

	PCR	PIR	Prime	All
Levene's Test	0.066	0.031	0.512	0.059
ANOVA	0.647	0.949	0.839	0.05
Welch	–	0.922	–	0.039

A.4. FT-IR

Table 6
Comparisons of intensities of characteristic PC peak (1775 cm^{-1}) normalized by the ABS characteristic peak (697 cm^{-1})

Ratio of peaks at **1775 cm-1/697 cm-1**	Sample 1	Sample 2	Sample 3	AVG
Prime94	0.493	0.594	0.630	0.572
Prime95	0.608	0.564	0.631	0.601
Prime96	0.613	0.605	0.586	0.601
PIR97	0.600	0.594	0.552	0.582
PIR98	0.552	0.585	0.648	0.595
PIR99	0.610	0.638	0.655	0.635
PCR27	1.030	0.976	0.988	0.998
PCR28	0.878	0.988	0.965	0.943
PCR45	0.848	0.812	0.850	0.837

Table 7
Comparisons of intensities of characteristic PC peak (829 cm^{-1}) normalized by the ABS characteristic peak (697 cm^{-1}) with tested batch density, estimated PC-ABS% and actual PC-ABS content

	IR PC	Density	Density Estimated
	peak Intensity	**(g/cm^3)**	**PC to ABS%**
Prime94	0.518	1.120	50/50
Prime95	0.506	1.117	48/52
Prime96	0.509	1.117	48/52
PIR97	0.515	1.119	49/51
PIR98	0.517	1.120	50/50
PIR99	0.546	1.122	52/48
PCR27	0.823	1.140	65/35
PCR28	0.815	1.141	65/35
PCR45	0.709	1.129	55/45

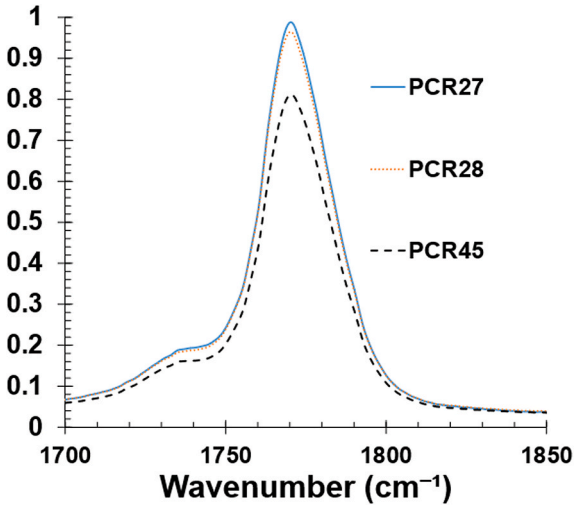

Fig. 10. Normalized ATR FT-IR spectra of PCR PC-ABS, with the 1775 cm^{-1} region expanded.

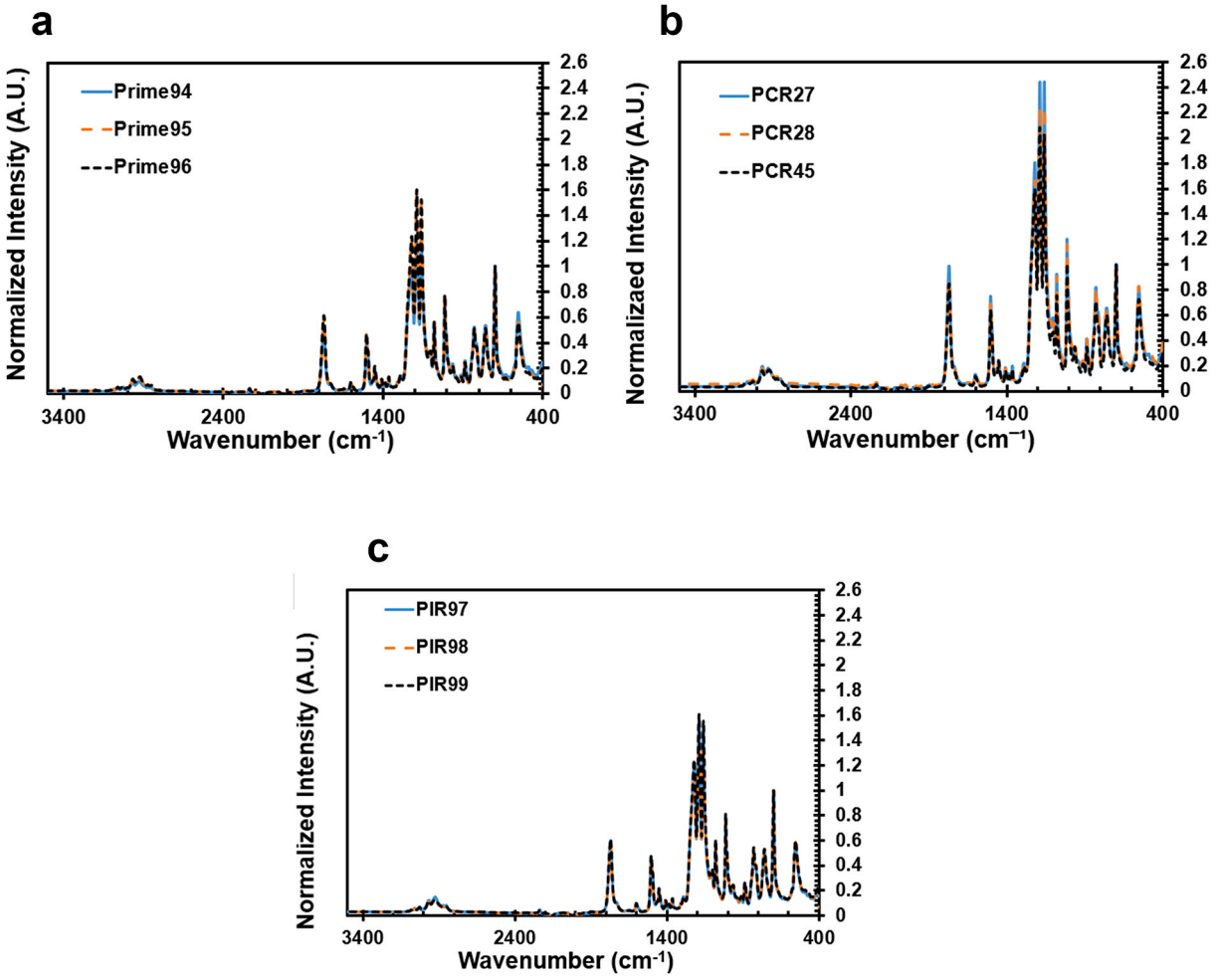

Fig. 11. Representative normalized FT-IR spectra of Prime (a), PIR (b) and PCR (c) polymers. Observable PC characteristic peaks are (cm^{-1}): 3010–3110: axial deformation aromatic C–H, 1770: axial deformation C═O, 829: angular deformation aromatic C–H [28]. Observable ABS characteristic peaks are (cm^{-1}): 3010–3110: axial deformation aromatic C–H, 1602: axial strain C═N, 697: aromatic C–H out of plane angular deformation [28].

Funding

This work was supported and funded by the Material Center and the CAE group at Volvo Cars.

Author Contribution Statement

Eliott Orzan: Investigation, Formal analysis, Writing – original draft. Ratchawit Janewithayapun: Investigation, Formal analysis, Writing – original draft. Renaud Gutkin: Writing – review & editing, Supervision, Corresponding Author. Giada Lo Re: Writing – review & editing, Supervision. Kai Kallo: Methodology, Resources, Writing – review & editing, Supervision.

References

[1] European Commision, A European strategy for plastics in a circular economy, Tech. Rep. (2018) 12.
[2] PlasticsEurope, Plastics – the facts 2019, Tech. Rep. (2019) 20–21. https://www.plasticseurope.org/download_file/force/3183/181.
[3] J. Hopewell, R. Dvorak, E. Kosior, Plastics recycling: challenges and opportunities, Philos. Trans. R. Soc. Lond. Ser. B Biol. Sci. 364 (1526) (2009) 2115–2126, https://doi.org/10.1098/rstb.2008.0311. ISSN 1471-2970, https://pubmed.ncbi.nlm.nih.gov/19528059 https://www.ncbi.nlm.nih.gov/pmc/articles/PMC2873020/.
[4] M. Villalobos, A. Awojulu, T. Greeley, G. Turco, G. Deeter, Oligomeric chain extenders for economic reprocessing and recycling of condensation plastics, Energy 31 (15) (2006) 3227–3234, https://doi.org/10.1016/j.energy.2006.03.026. ISSN 0360-5442, http://www.sciencedirect.com/science/article/pii/S0360544206000079X.
[5] H. Suarez, J.W. Barlow, D.R. Paul, Mechanical properties of ABS/polycarbonate blends, J. Appl. Polym. Sci. 29 (11) (1984) 3253–3259, https://doi.org/10.1002/app.1984.070291104. ISSN 0021-8995.
[6] J. Li, F. Chen, L. Yang, L. Jiang, Y. Dan, FTIR analysis on aging characteristics of ABS/PC blend under UV-irradiation in air, Spectrochim. Acta Mol. Biomol. Spectrosc. 184 (2017) 361–367, https://doi.org/10.1016/j.saa.2017.04.075. ISSN 13861425.
[7] R. Greco, M.F. Astarita, L. Dong, A. Sorrentino, Polycarbonate/ABS blends: processability, thermal properties, and mechanical and impact behavior, Adv. Polym. Technol. 13 (4) (1994) 259–274, https://doi.org/10.1002/adv.1994.060130402. ISSN 0730-6679.
[8] V.V. Rajan, R. Wäber, J. Wieser, Influence of different types of UV absorber/UV stabilizer combination on the photodegradation of PC/ABS blend, J. Appl. Polym. Sci. 124 (5) (2012) 4007–4015, https://doi.org/10.1002/app.34560. ISSN 00218995.
[9] H. T. Chiu, J. K. Huang, M. T. Kuo, J. H. Huang, Characterisation of PC/ABS blend during 20 reprocessing cycles and subsequent functionality recovery by virgin additives, J. Polym. Res. 25 (5), ISSN 15728935, doi:10.1007/s10965-018-1522-6..
[10] A. Ram, O. Zilber, S. Kenig, Life expectation of polycarbonate, Polym. Eng. Sci. 25 (9) (1985) 535–540, https://doi.org/10.1002/pen.760250905. https://onlinelibrary.wiley.com/doi/abs/10.1002/pen.760250905.

[11] M. Diepens, P. Gijsman, Photo-oxidative degradation of bisphenol A polycarbonate and its possible initiation processes, Polym. Degrad. Stabil. 93 (7) (2008) 1383–1388, https://doi.org/10.1016/j.polymdegradstab.2008.03.028, 01413910.
[12] D. Schönmayr, Automotive plastics and sustainability, in: Automotive Recycling, Plastics, and Sustainability: the Recycling Resistance, Springer International Publishing, 2017, pp. 54–69, chap. 3.
[13] A. Farzadfar, S.N. Khorasani, S. Khalili, Blends of recycled polycarbonate and acrylonitrile-butadiene-styrene: comparing the effect of reactive compatibilizers on mechanical and morphological properties, Polym. Int. 63 (1) (2014) 145–150, https://doi.org/10.1002/pi.4493, 09598103.
[14] X. Liu, H. Bertilsson, Recycling of ABS and ABS/PC blends, J. Appl. Polym. Sci. 74 (3) (1999) 510–515, https://doi.org/10.1002/(SICI)1097-4628(19991017)74:3<510::AID-APP5>3.0.CO 2-6. ISSN 0021-8995.
[15] D. Mahanta, S.A. Dayanidhi, S. Mohanty, S.K. Nayak, Mechanical, thermal, and morphological properties of recycled polycarbonate/recycled poly(acrylonitrile-butadiene-styrene) blend nanocomposites, Polym. Compos. 33 (12) (2012) 2114–2124, https://doi.org/10.1002/pc.22342. ISSN 15480569.
[16] V. Ramesh, M. Biswal, S. Mohanty, S.K. Nayak, Compatibilization effect of EVA-g-MAH on mechanical, Morphological and rheological properties of recycled PC/ABS blend, Materials Express 4 (6) (2014) 499–507, https://doi.org/10.1166/mex.2014.1198. ISSN 21585857.
[17] M.B. Brown, A.B. Forsythe, Robust tests for the equality of variances, J. Am. Stat. Assoc. 69 (346) (1974) 364–367, https://doi.org/10.1080/01621459.1974.10482955. ISSN 0162-1459, https://www.tandfonline.com/doi/abs/10.1080/01621459.1974.10482955.
[18] M. Hallahan, R. Rosenthal, 5 - Interpreting and Reporting Results, Academic Press, San Diego, 2000, ISBN 978-0-12-691360-6, https://doi.org/10.1016/B978-012691360-6/50006-9. http://www.sciencedirect.com/science/article/pii/B9780126913606500069.
[19] K. Yeager, P. Bhattacharya, V. Reynolds, SPSS tutorials. https://libguides.library.kent.edu/SPSS, 2015.
[20] R. D'Agostino, E.S. Pearson, Tests for departure from normality, Biometrika 60 (3) (1973) 613–622, https://doi.org/10.2307/2335012. ISSN 00063444, http://www.jstor.org/stable/2335012.
[21] S.S. Shapiro, M.B. Wilk, An analysis of variance test for normality (complete samples), Biometrika 52 (3/4) (1965) 591–611, https://doi.org/10.2307/2333709. ISSN 00063444, http://www.jstor.org/stable/2333709.
[22] ISO, ISO 527-2:2012, tech. Rep, 2017, https://www.iso.org/standard/56046.html, 2017.
[23] R.E. Evans, D.R. Ireland, Physical Testing of Plastics: Correlation with End-Use Performance, ASTM International, 1981.
[24] G.M. Swallowe, Mechanical Properties and Testing of Polymers : an A-Z Reference, Springer Netherlands, 1999, ISBN 9789048140244.
[25] P. Virtanen, R. Gommers, T.E. Oliphant, M. Haberland, T. Reddy, D. Cournapeau, E. Burovski, P. Peterson, W. Weckesser, J. Bright, S.J. van der Walt, M. Brett, J. Wilson, K.J. Millman, N. Mayorov, A.R.J. Nelson, E. Jones, R. Kern, E. Larson, C. J. Carey, I. Polat, Y. Feng, E.W. Moore, J. VanderPlas, D. Laxalde, J. Perktold, R. Cimrman, I. Henriksen, E.A. Quintero, C.R. Harris, A.M. Archibald, A.H. Ribeiro, F. Pedregosa, P. van Mulbregt, A. Vijaykumar, A.P. Bardelli, A. Rothberg, A. Hilboll, A. Kloeckner, A. Scopatz, A. Lee, A. Rokem, C.N. Woods, C. Fulton, C. Masson, C. Häggström, C. Fitzgerald, D.A. Nicholson, D.R. Hagen, D. V. Pasechnik, E. Olivetti, E. Martin, E. Wieser, F. Silva, F. Lenders, F. Wilhelm, G. Young, G.A. Price, G.-L. Ingold, G.E. Allen, G.R. Lee, H. Audren, I. Probst, J. P. Dietrich, J. Silterra, J.T. Webber, J. Slavič, J. Nothman, J. Buchner, J. Kulick, J. L. Schönberger, J.V. de Miranda Cardoso, J. Reimer, J. Harrington, J.L. C. Rodríguez, J. Nunez-Iglesias, J. Kuczynski, K. Tritz, M. Thoma, M. Newville, M. Kümmerer, M. Bolingbroke, M. Tartre, M. Pak, N.J. Smith, N. Nowaczyk, N. Shebanov, O. Pavlyk, P.A. Brodtkorb, P. Lee, R.T. McGibbon, R. Feldbauer, S. Lewis, S. Tygier, S. Sievert, S. Vigna, S. Peterson, S. More, T. Pudlik, T. Oshima, T.J. Pingel, T.P. Robitaille, T. Spura, T.R. Jones, T. Cera, T. Leslie, T. Zito, T. Krauss, U. Upadhyay, Y.O. Halchenko, Y. Vázquez-Baeza, S. Contributors, SciPy 1.0: fundamental algorithms for scientific computing in Python, Nat. Methods 17 (3) (2020) 261–272, https://doi.org/10.1038/s41592-019-0686-2. ISSN 1548-7105.
[26] M. M. Khan, R. Liang, R. Gupta, S. Agarwal, Rheological and mechanical properties of ABS/PC blends, Korea-Australia rheology J. 17..
[27] I. Nigam, D. Nigam, G.N. Mathur, Effect of rubber content of ABS on properties of PC/ABS blends. I. Rheological, mechanical, and thermal properties, Polym. Plast. Technol. Eng. 44 (5) (2005) 815–832, https://doi.org/10.1081/PTE-200060828. ISSN 03602559.
[28] A.C. Ferreira, M.F. Diniz, E.d.C. Mattos, FT-IR Methodology (Transmission and UATR) to Quantify Automotive Systems, 2018, https://doi.org/10.1590/0104-1428.2412.
[29] T. Seelig, E. Giessen, Effects of microstructure on crack tip fields and fracture toughness in PC/ABS polymer blends, Int. J. Fract. 145 (3) (2007) 205–222, https://doi.org/10.1007/s10704-007-9117-y. ISSN 03769429.
[30] K.G. Pijnenburg, A.C. Steenbrink, E.V.D. Giessen, Shearing of particles during crack growth in polymer blends, Polymer 40 (21) (1999) 5761–5771, https://doi.org/10.1016/S0032-3861(98)00780-0, 00323861.
[31] W. Cox, E. Merz, Understanding Rheology of Thermoplastic Polymers, 2013.
[32] M. Ansari, S. Hatzikiriakos, A. Sukhadia, D. Rohlfing, Rheology of Ziegler-Natta and metallocene high-density polyethylenes: broad molecular weight distribution effects, Rheol. Acta 50 (2011) 17–27, https://doi.org/10.1007/s00397-010-0503-4.
[33] S. Aid, A. Eddhahak, Z. Ortega, D. Froelich, A. Tcharkhtchi, Experimental study of the miscibility of ABS/PC polymer blends and investigation of the processing effect, J. Appl. Polym. Sci. 134 (25), ISSN 0021-8995, doi:10.1002/app.44975, URL https://doi.org/10.1002/app.44975.
[34] M. Fatih Ergin, I. Aydin, Evaluation of rheological behaviour upon recycling of an ethylene vinyl acetate copolymer by means of twin-screw extrusion process, in: Acta Physica Polonica A, vol. 131, Polish Academy of Sciences, 2017, pp. 542–544, https://doi.org/10.12693/APhysPolA.131.542, 1898794X.
[35] International Standard, 2000. ISO 6603-2:2000(E), Tech. Rep. https://www.sis.se/std-616872.
[36] S.W.F. Spronk, M. Kersemans, J.C.A. De Baerdemaeker, F.A. Gilabert, R.D. B. Sevenois, D. Garoz, C. Kassapoglou, W. Van Paepegem, Comparing damage from low-velocity impact and quasi-static indentation in automotive carbon/epoxy and glass/polyamide-6 laminates, Polym. Test. 65 (2018) 231–241, https://doi.org/10.1016/j.polymertesting.2017.11.023. ISSN 0142-9418, http://www.sciencedirect.com/science/article/pii/S0142941817315660.
[37] A. Nettles, M. Douglas, A Comparison of Quasi-Static Indentation to Low-Velocity Impact, ASTM Special Technical Publication ..
[38] A. Highsmith, A Study of the Use of Contact Loading to Simulate Low Velocity Impact, 1997.
[39] S.M. Lee, P. Zahuta, Instrumented impact and static indentation of composites, J. Compos. Mater. 25 (2) (1991) 204–222, https://doi.org/10.1177/002199839102500205. ISSN 0021-9983.
[40] G.M. Swallowe, Yield and plastic deformation, in: G.M. Swallowe (Ed.), Mechanical Properties and Testing of Polymers: an A-Z Reference, Springer Netherlands, Dordrecht, 1999, pp. 281–285, https://doi.org/10.1007/978-94-015-9231-4_61. ISBN 978-94-015-9231-4.